

## Article

# Effects of Unbalanced Incentives on Threshing Drum Stability during Rice Threshing

Kexin Que <sup>1</sup>, Zhong Tang <sup>1,2,\*</sup> , Ting Wang <sup>3</sup>, Zhan Su <sup>4</sup>  and Zhao Ding <sup>4</sup>

<sup>1</sup> School of Agricultural Engineering, Jiangsu University, Zhenjiang 212013, China; 3222502002@stmail.ujs.edu.cn

<sup>2</sup> Key Laboratory of Intelligent Equipment and Robotics for Agriculture of Zhejiang Province, Hangzhou 310058, China

<sup>3</sup> Jiangsu World Agriculture Machinery Co., Ltd. (WORLD A/M), Zhenjiang 212311, China; 15996802195@163.com

<sup>4</sup> Key Laboratory of Crop Harvesting Equipment Technology of Zhejiang Province, Jinhua 321017, China; sz\_627@126.com (Z.S.); dingzhao0806@foxmail.com (Z.D.)

\* Correspondence: zht@ujs.edu.cn

**Abstract:** As a result of the uneven growth of rice, unbalanced vibration of threshing drum caused by stalk entanglement in combine harvester is more and more severe. In order to reveal the influence of unbalanced excitation on the roller axis locus during rice threshing, the stability of threshing drum was studied. The dynamic signal test and analysis system are used to test the axial trajectory of threshing drum. At the same time, the influence of the unbalanced excitation caused by the axis winding on the axis trajectory is analyzed by the experimental results. Axis locus rules under no-load and threshing conditions are obtained. In order to simulate the axial and radial distribution of unbalanced excitation along the threshing drum, the counterweight was distributed on the threshing drum instead of the entangled stalk. Then, the definite effect of unbalanced excitation on the rotating stability of threshing drum is analyzed. Results show that the amplitude of stem winding along the grain drum is larger in the vertical direction and smaller in the horizontal direction when compared with the unloaded state under 200 g weight. It was found that the amplitude in both horizontal and vertical directions decreased after 400 g and 600 g counterweights were added, respectively, to simulate the radial distribution of stalk winding along the grain barrel. Finally, it can be seen that with the increase in the weight of the counterweight, the characteristics of the trajectory misalignment of the threshing cylinder axis become more and more obvious. This study can provide reference for reducing the unbalanced excitation signal of threshing drum and improving driving comfort.

**Keywords:** threshing cylinder; axis locus; amplitude; counterweight block; unbalanced excitation



**Citation:** Que, K.; Tang, Z.; Wang, T.; Su, Z.; Ding, Z. Effects of Unbalanced Incentives on Threshing Drum Stability during Rice Threshing. *Agriculture* **2024**, *14*, 777. <https://doi.org/10.3390/agriculture14050777>

Academic Editor: Alessio Cappelli

Received: 17 April 2024

Revised: 4 May 2024

Accepted: 12 May 2024

Published: 17 May 2024



**Copyright:** © 2024 by the authors. Licensee MDPI, Basel, Switzerland. This article is an open access article distributed under the terms and conditions of the Creative Commons Attribution (CC BY) license (<https://creativecommons.org/licenses/by/4.0/>).

## 1. Introduction

With the increase in rice yield, the unbalanced incentive caused by rice stalk entanglement in the harvest process is still accompanied by the whole threshing process and changeable, which is easy to shorten the life of the threshing drum. In the process of threshing, the threshing drum vibration phenomenon constantly disappeared by the end of the threshing process. The vibration of threshing drum will not only affect its own threshing performance, but also cause structural resonance of the frame, vibrating screen, fan, return plate, etc., affecting the structural reliability of the machinery and making the machine noise higher [1]. At the same time, it can also affect the driver's sense of driving [2]. According to statistics, about 60% of excessive vibration in rotating machinery is related to misalignment. Force imbalance is the main factor leading to the misalignment of rotating machinery, and the unbalanced excitation of threshing device will affect the axis trajectory of the central axis of the threshing drum.

The threshing drum is generally in a stable running state under no-load condition. However, the cylinder contains a cylindrical shell structure, which is easy to produce eccentric rotation, resulting in changes in the axis locus. By analyzing the buckling and free vibration of the eccentric rotating cylindrical shell under axial excitation, the natural frequency of the eccentric rotating cylindrical shell can be obtained [3]. By comparing the natural frequency under different conditions with the numerical modal analysis results, it is found that the natural frequency is of a higher order [4]. The change in rotor speed caused by eccentric rotation not only changes the frequency of vibration components [5], but also converts the dynamic rotor vibration energy of eccentric mass into electrical energy [6]. Permanent magnet motors with increased mechanical power will also be disturbed by unbalanced vibration [7]. Therefore, the off-center rotation of the threshing drum still exists under no-load condition, which causes the trajectory of the threshing drum axis to change.

Ensuring stable and uniform feeding of rice into the threshing separation device before threshing can improve the working quality of the threshing drum [8]. In the threshing process, the straw wrapped around the threshing drum will inevitably lead to incentive imbalance, and the grain bears the threshing load during the threshing process [9]. The unbalanced excitation of the threshing drum not only comes from the winding of straw, but also the state excitation signal of the continuous roller bearing used for threshing in the threshing drum device will cause the central trajectory of the central axis of the threshing drum to change [10]. In order to observe the change in the central trajectory more accurately, vibration changes on threshing cylinders are detected with a monitoring system [11]. In addition, relevant studies have shown that the wear rate of threshing drum can be reduced by changing suitable materials [12]. An approximate solution can be obtained by associating the variables of stalks of different lengths and thickness in the threshing process [13]. The influence of the mixture on the threshing separation effect can be deduced [14], and the threshing process can be predicted by using the particle motion velocity [15], and the predicted results can be compared with the experimental results. The performance evaluation of the drum in threshing process was obtained [16].

Unbalanced vibration not only affects the mechanical stability and reliability of agricultural machinery, but also dynamically changes the behavior of rail components due to the unbalanced mass in road construction [17]. Eccentricity defects lead to changes in the critical fluid velocity of pipelines [18]. Moreover, the parameters of the threshing drum are still uncertain; therefore, a multi-objective optimization technique is needed to estimate these unknowns [19], and the fault detection and solution of the mixed eccentricity of the rotor can be performed through diagnostic methods [20]. In the process of rice harvesting, stem entanglement can cause incentive imbalance and affect driving comfort. In order to improve the driving comfort of the driver, the influence of unbalanced excitation on the rotating stability of the threshing drum is reduced. The threshing drum under vertical vibration was modeled and evaluated [21], and then appropriate parameters were set to verify the performance evaluation of the threshing drum through the threshing drum [22]. Therefore, unbalanced excitation affects all aspects; thus it is more important to study the influence of unbalanced excitation on the rotating stability of the drum.

In order to study the influence of unbalanced excitation on the rotating stability of rice threshing drum, this paper takes the axis locus as the characterization of the rotating stability of the drum in the test. The shaft end vibration of threshing drum under no-load and threshing conditions was respectively detected, and then the influence of unbalanced excitation caused by stalk winding on the axis locus was tested. On the basis of the test results, the winding state of rice stalk on threshing rod teeth was simulated by adding counterweight to threshing rod teeth. The influence of uneven distribution of rice stalk along the roller on the vibration characteristics of the roller was studied by monitoring the track of the roller. The distribution of eccentric mass on the roller was more accurately studied, and the law of influence of unbalanced excitation on the track of the roller center axis was analyzed. This research can provide a basis for reducing the unbalanced excitation

of the drum in the threshing process, improving the rotation stability of the drum and improving the driving sense of the driver.

## 2. Material and Methods

### 2.1. Materials and Test Equipment

#### (1) Structure and parameters of threshing drum

The threshing drum device is the main working part of the grain threshing task, which is composed of rotating threshing drum, top cover, and concave screen. Among them, the grid concave screen is located in the lower part of the threshing drum device, and the top cover is located in the upper part of the threshing drum. The axial threshing drum is installed in the space formed by the grid concave plate screen and the top cover. The three-dimensional modeling of the threshing drum using Pro/E is shown in Figure 1. It can be seen from the structure that the threshing drum has a symmetrical structure, which means that the threshing drum does not exist in the structure of the drum imbalance. After rice enters the concave plate sieve, the threshing roller and the concave plate sieve interact with each other through friction, impact, brushing and extrusion, so as to realize the threshing separation of rice. In the working process of the threshing drum, the threshing mainly depends on the impact of the nail teeth on the material and rubbing.

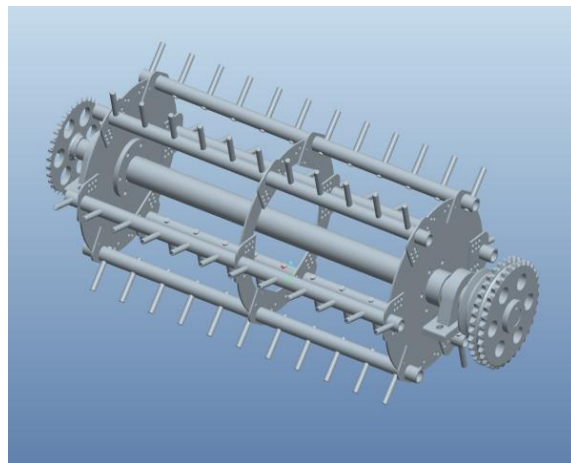


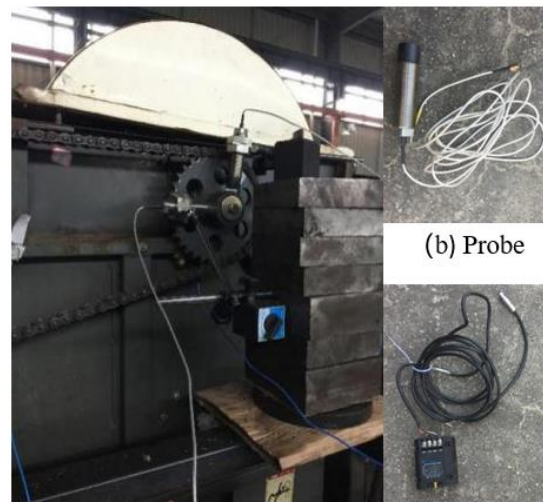
**Figure 1.** Dimensional modeling of threshing drum.

The threshing drum used in this paper has a threshing gap of 15–25 mm, the diameter of the threshing drum is 360 mm, the working speed is  $800 \text{ r}\cdot\text{min}^{-1}$ , and the peak speed is  $760 \text{ r}\cdot\text{min}^{-1}$ . The material properties of the threshing drum device are set according to the manufacturing material of the drum. The main body of the threshing drum is made of Q235-A ordinary carbon structural steel. Q235-A ordinary carbon structural steel is from Liaocheng Mingkang Metal Materials Co., Ltd., Liaocheng, Shandong, China. The density of the material is  $7.85 \text{ g}\cdot\text{cm}^{-3}$ , the yield strength is 225 MPa, the allowable shear stress is 15–25 MPa, and the allowable bending stress is 40 MPa. These parameters can better improve threshing efficiency and reduce damage to rice [23].

#### (2) Signal acquisition system and instrument

DH5902 dynamic signal test and analysis system of Donghua Test Company (Taizhou, China) were used in the test. Among them, DH5902 dynamic signal test system comes from Jiangsu Donghua Test Technology Co., Ltd., Taizhou, China. The hardware of the system includes DH5902 signal acquisition instrument and eddy current displacement sensor. The eddy current displacement sensor can measure the displacement curve of the threshing drum surface along the measurement direction of the probe with time. The two sensors are vertically distributed to each other, while the control eddy current sensor is fixed at 3 mm–5 mm outside the shaft end of the threshing drum, so as to accurately describe the

axis trajectory of the threshing drum. The arrangement and fixing of the sensor in the test are shown in Figure 2, where the eddy current displacement sensor is composed of a probe and a preprocessor.



(a) Eddy current sensor field layout (c) Preprocessor

**Figure 2.** Materials required for eddy current sensors.

The main performance parameters of the test instrument are shown in Table 1. In the material, the 5E104 eddy current displacement sensor comes from Jiangsu Donghua Test Technology Co., Ltd. in Taizhou, Shandong Province, China. In order to ensure the normal operation of the threshing drum, Jotautienė et al. studied the rolling bearing condition of the threshing drum of a combine harvester that was difficult to access through vibration diagnosis technology [24].

**Table 1.** Test instrument main performance parameters.

Device Name	Technical Index	Parameter Value
5E104 Eddy current displacement sensor	Sensitivity (V/mm)	1.7
	Range (mm)	6
	Nonlinear error (%)	±1%
	Probe diameter (mm)	φ25
	Excitation voltage (Vdc)	±15
	Operating temperature (°C)	−20–120
	Frequency range (Hz)	0–10,000
DH5902 Rugged data acquisition system	Sampling rate	Maximum 256 Hz/channel
	Number of channels	32
	Impact resistance (g/ms)	100 g/(4 ± 1 ms)

To ensure that the two eddy current sensors are perpendicular to each other, the two sensors are fixed in the vertical direction and the horizontal direction, respectively. In fact, as long as the perpendicular direction between the two sensors can meet the test requirements, the sensors can be fixed in any direction.

### (3) Axis locus measurement method

Threshing drum is a kind of rotating machinery, the axis locus is one of the contents of time-domain analysis of its vibration signal. Different kinds of threshing rollers reflect different motion states. The axis track of rotating machinery is usually elliptical, but under the interference of frequency doubling, harmonics and other components, the track will become uneven and tortuous. Even if a rotor system runs for a long time, its trajectory curves can not only achieve overlap, but also the distribution range of the axis locus is relatively concentrated. When the track lines are no longer overlapping, namely, the

distribution area and shape repeatability of the track lines are poor, it is necessary to analyze the vibration time domain curve of the rotating sub-system to find out the factors leading to the instability of the operating state. Fukushima et al. proposed a method of constructing rotor axis locus based on the coordinates of each frequency component to investigate rotor vibration characteristics in detail, and observed the phenomenon of nonlinear vibration of the rotor through this method [25]. Since the vibration of the threshing drum is nonlinear when it is wrapped by straw, the change in the trajectory curve of the central axis can be obtained by this method.

When synthesizing the axis locus, ensure that X and Y are marked in the same direction as the eddy current sensor. By synthesizing the time-domain signals measured by the two sensors, the axis locus diagram of the threshing drum can be obtained. Due to the shape error of the measured axis end, and the fact that the threshing drum cannot completely adjust the medium factors after installation, the data measured by the time-domain signal are not only the offset heartbeat momentum caused by rice stalk entanglement.

Since the surface of the central axis of the threshing drum has a shape error, the horizontal component and vertical component are respectively  $S_x$  and  $S_y$ , then the instantaneous time-domain signal collected by the eddy current sensors 1 and 2 can be expressed as follows:

$$\begin{cases} r_x = S_x + f_x + e_x \\ r_y = S_y + f_y + e_y \end{cases} \quad (1)$$

Equation (1) can be more directly illustrated by Figure 3. Since the instantaneous runout vector caused by the winding of rice stems is much larger than the shape error of the central axis and the initial eccentricity of the threshing drum,  $S$  and  $e$  in Equation (1) can be ignored in the analysis below.

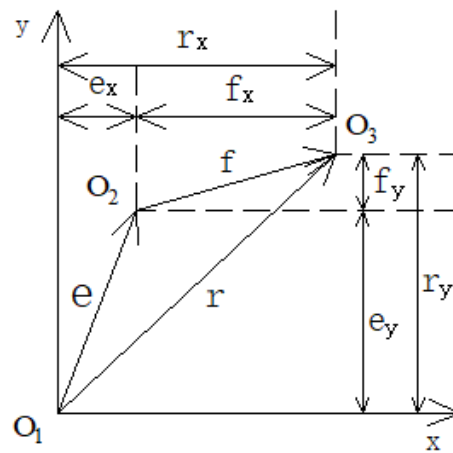


Figure 3. Time-domain signal analysis local diagram.

By synthesizing the time-domain signals measured by the two sensors, the axis locus diagram of the threshing drum can be obtained. Considering the shape error of the measured axis end and the fact that the threshing drum cannot completely adjust the medium factor after installation, the data measured by the time-domain signal are more than the eccentric heartbeat momentum caused by rice stalk entanglement. The time-domain signal analysis diagram is shown in Figures 3 and 4. In Figures 3 and 4,  $O_1$  is the average rotation center of the central axis of the threshing drum,  $O_2$  is the rotation axis of the central axis of the threshing drum,  $O_3$  is the instantaneous rotation axis of the central axis of the threshing drum,  $e$  is the initial eccentricity of the central axis of the threshing drum, and  $f$  is the instantaneous beating vector of the central axis of the threshing drum during rotation. Additionally,  $r$  is the position vector of the instantaneous rotation axis  $O_3$ .

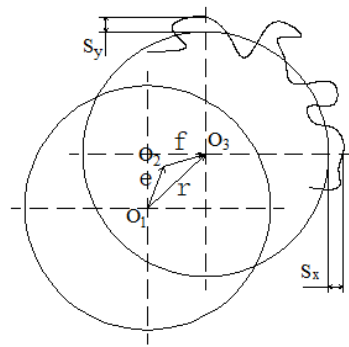


Figure 4. Time-domain signal analysis diagram.

In order to reveal that a haulm wound caused by unbalanced vibration, respectively by the no-load and threshing state for a period of time-domain vibration signal analysis, a contrast analysis stem wound caused by unbalanced vibration affects the axis path.

2.2. Test Method

(1) Stalk winding state model

A finite element analysis of the unbalanced tension of the generator with and without damped windings has shown that the eccentricity of the sheller drum would cause losses [26]. In addition, depending on the gyroscope effect, these loads may temporarily increase ten-fold as the machine rotates [27]. For accurate analysis, the finite element method can be used to analyze the mode of the closed thin-walled cylindrical shell. It is found that the cylinder stability of the cylindrical shell is better when the flat end face is used [28]. At the same time, the stalks are damaged during the threshing process [29,30]. Some relevant researchers have optimized the combine harvester and significantly reduced the threshing loss rate [31–33]. The fault detection of combine harvester is also indispensable [34].

Next, we study the effect of rice stem on the threshing drum when it is running under no-load condition. Ax and Ay are the motion amplitudes of the central axis of the threshing drum in the x and y directions, respectively. φx and φy are the phase angles of motion in the x and y directions, respectively; therefore, the equation of the axis motion can be expressed as follows:

$$\begin{cases} x = A_x \cos(\omega t + \varphi_x) \\ y = A_y \sin(\omega t + \varphi_y) \end{cases} \tag{2}$$

By expanding the trigonometric function in Equation (2), we can obtain the following:

$$\begin{cases} x = A_x \cos(\omega t) \cos \varphi_x - A_x \sin(\omega t) \sin \varphi_x \\ y = A_y \sin(\omega t) \cos \varphi_y + A_y \cos(\omega t) \sin \varphi_y \end{cases} \tag{3}$$

Then, the following order:

$$\begin{cases} X_c = A_x \cos \varphi_x \\ X_s = A_x \sin \varphi_x \\ Y_c = A_y \sin \varphi_y \\ Y_s = -A_y \cos \varphi_y \end{cases} \tag{4}$$

Then, we can obtain:

$$\begin{cases} A_x = \sqrt{X_c^2 + X_s^2} \\ A_y = \sqrt{Y_c^2 + Y_s^2} \\ \tan \varphi_x = \frac{X_s}{X_c} \\ \tan \varphi_y = -\frac{Y_c}{Y_s} \end{cases} \tag{5}$$

The final Equations (5) can be derived as follows:

$$\begin{cases} x = X_c \cos(\omega t) - X_s \sin(\omega t) \\ y = Y_c \cos(\omega t) - Y_s \sin(\omega t) \end{cases} \quad (6)$$

Equation (6) is the expression of the axis locus of the central axis of the threshing drum under no-load condition. It can be seen from Equation (6) that the axis locus of the central axis of the threshing drum under no-load condition is elliptical.

According to Figure 5, it can be seen that when the threshing drum is working, a large number of rice stalks will be wrapped between the threshing rod teeth and the central axis, resulting in eccentric additional mass inside the drum. On the combine harvester, the unbalance of the threshing drum has a great impact on the quality of its cooperation. The threshing drum will produce a large unbalance force when it turns eccentrically, which will increase the pressure on the bearings at both ends of the threshing drum, making the bearings suffer from wear. The uneven axial and radial distribution of rice stalks along the threshing drum can be analyzed through Figures 6 and 7. The mass eccentricity of the threshing drum and the rice stalk leads to an imbalance in the drum, with the unbalanced force being the centrifugal force that causes the stalk to wrap around the drum.



**Figure 5.** A winding stalk on a threshing drum.

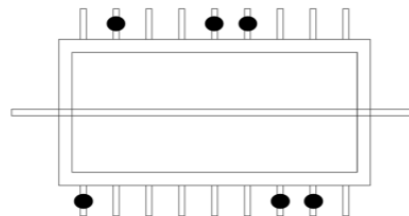


**Figure 6.** Main view of stalk winding state.

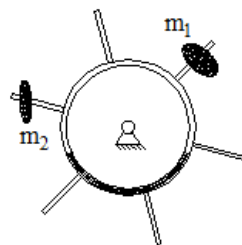


**Figure 7.** Side view of stalk winding state.

In the process of rice threshing, the stalks are often wound on the teeth of the threshing rod. After the threshing drum is stopped abruptly and the top cover of the threshing drum is opened, the winding state of rice on the threshing drum can be observed, as shown in Figure 5. The schematic diagram is drawn according to the winding state of the rice stalk on the threshing drum, as shown in Figure 7, where  $m_1$  and  $m_2$  represent the winding mass of the stalk in multiple phases.

## (2) Axial unbalance excitation test of threshing drum

In the initial stage of rice feeding, rice is constantly fed from the feeding end into the threshing drum and moves towards the grass discharging end. The continuous increase in stalk mass on the threshing rod teeth is similar to the continuous increase in counterweight. Meanwhile, the uneven distribution of rice along the threshing drum will enhance the unbalanced vibration of the threshing drum. Lim et al. simulated the free vibration and forced vibration characteristics of the whole rotor system by the finite element method, designed an artificial intelligence feedback controller, and finally proved the reliability of the intelligent feedback controller [35]. In a study by Huynh et al., based on the assumption that grain threshing separation meets exponential distribution, a threshing separation probability model was established [36]. Therefore, it is reliable to use counterweight blocks to simulate stalk winding in this paper. In order to understand the influence of unbalanced excitation on the axis trajectory of threshing drum more accurately, this paper uses counterweight to simulate rice straw, which is divided into two kinds of tests: axial distribution and radial distribution.

Since the axial trajectory can be used as a characteristic signal to identify the misalignment of rotor effectively, it has been widely used in rotor dynamics. Therefore, the axis locus of threshing drum is used as the characteristic signal to study its eccentricity. Under the influence of the degradation of the rice feeding amount with time, the uneven winding of straw on the threshing rod teeth and the continuous loss of grains during the movement from the rice feeding end to the weeding end, the threshing drum will produce unbalanced excitation during the threshing process, and the unbalanced state will constantly change. As it is difficult to quantitatively adjust the quality of rice stalk wrapped on the threshing drum, this paper uses counterweight to quantitatively lead rice stalk to simulate the rice stalk wrapped on the threshing drum for experimental research.

In order to analyze the vibration state of threshing drum more accurately, rice stems were divided into axial and radial distribution states. Firstly, all the counterweights were fixed on the same row of threshing rod teeth of the threshing drum to simulate the changes in the axial distribution of rice stalks under the threshing condition. The test is divided into four groups, at the same time, some counterweights were prepared, weighing 100 g as shown in Figure 8. In the first group of tests, no counterweight was added to simulate the vibration state of threshing drum under no-load condition. Then, two counterweight blocks were added to each group successively to ensure that the counterweight blocks were added successively from the feeding end of threshing drum to the discharging end, so as to simulate the process of rice stalks moving from the feeding end of threshing drum to the discharging end, while the stalk mass gradually increased. It is used to investigate the influence of eccentric mass distribution along the threshing drum on the vibration characteristics of the threshing drum.

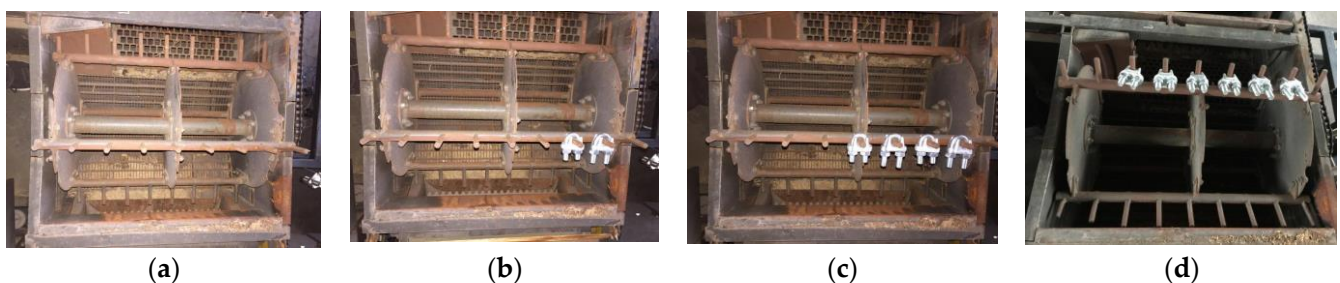


**Figure 8.** Tests to explore the distribution of eccentric mass along the axial direction. (a) No additional counterweight; (b) Add 200 g of breeding blocks; (c) Add 400 g of counterweight; (d) Add 600 g of counterweight.

The center of the eddy current sensor is fixed at the side of the rice feeding shaft end; in two kinds of small throttle with full throttle monitoring, the threshing cylinder axis

path changes. Therefore, to explore stem winding along the axis of cylinder of unbalanced distribution of threshing, the cylinder vibrations are studied.

### (3) Radial unbalance excitation test of threshing drum

In fact, when rice is threshed, the rice stalks are not only wound on the same row of threshing rod teeth, but spiral wound on the surface due to the rotation of the threshing drum; therefore, it is necessary to study the influence and law of the uneven radial winding of rice stalks along the threshing drum on the axis locus.

The eddy current displacement sensor is fixed near the water feeding inlet side of the shaft end, respectively; in two kinds of small throttle and big gas monitoring, the threshing cylinder axis path changes. The test was divided into four groups: the first group was distributed in a coaxial direction without adding a counterweight; the second group was fixed with a counterweight of 200 g on the moral side near the feeding end, and two counterweights were added successively in the following two groups, as shown in Figure 9.

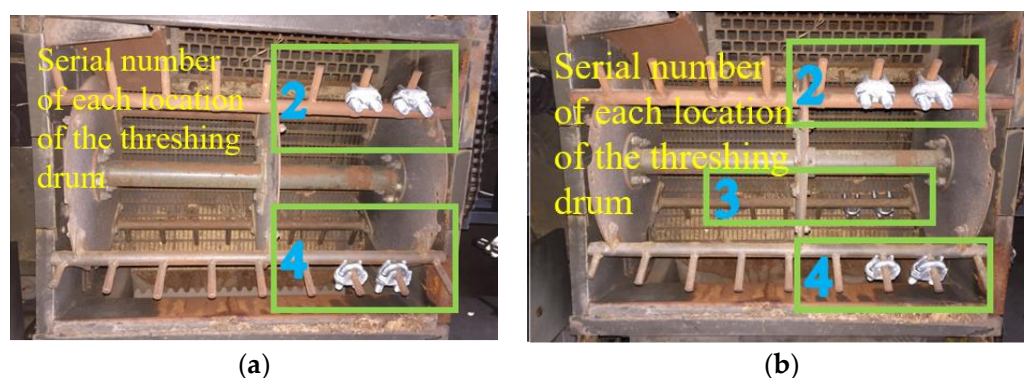


**Figure 9.** Tests to explore the radial distribution of eccentric mass. (a) Add 400 g counterweight (top cover 200 g, concave screen 200 g); (b) Add 600 g counterweight (200 g for top cover, 200 g for concave screen, 200 g between the top cover and concave screen).

## 3. Results and Discussion

### 3.1. Influence of Axial Unbalance of Stem Winding on Axis Locus of Threshing Drum

In the test process, the rotating speed of the threshing drum is controlled near 600 rpm; therefore, the rotation period of the threshing drum is about 0.1 s. In order to avoid the tracks crossing each other in a long period of time caused by the intricate axis tracks of the threshing drum, the axis tracks within 0.2 s and 1.0 s were intercepted for analysis, and the axis tracks were intercepted from the test results, as shown in Figure 10 without counterweight.

As can be seen in Figure 10, with a threshing cylinder with small throttle counterweight running state, the horizontal amplitude is 0.375 mm and the vertical amplitude is 0.900 mm, whereas with a large throttle state run time, the horizontal amplitude is 2.100 mm and the vertical direction of the moral amplitude increases to 1.400 mm. The axis tracks in the figure are scattered, there is no tendency to concentrate in one area, but it can still be seen that there are some spikes on the trajectory curve, indicating that the grain cylinder is in a stable running state on the whole. However, there is still friction in the local rotation.

According to Figure 11, it can be found that when 200 g counterweight is added to the threshing drum, the amplitude in the horizontal direction is about 0.300 mm and that in the vertical direction is 1.350 mm. In the condition of large gas, the horizontal amplitude increases to 1.500 mm and the vertical amplitude increases to 1.800 mm. The axis path and scattered distribution did not focus on the trend of a certain direction, which means that they appear in the wrong phenomenon.

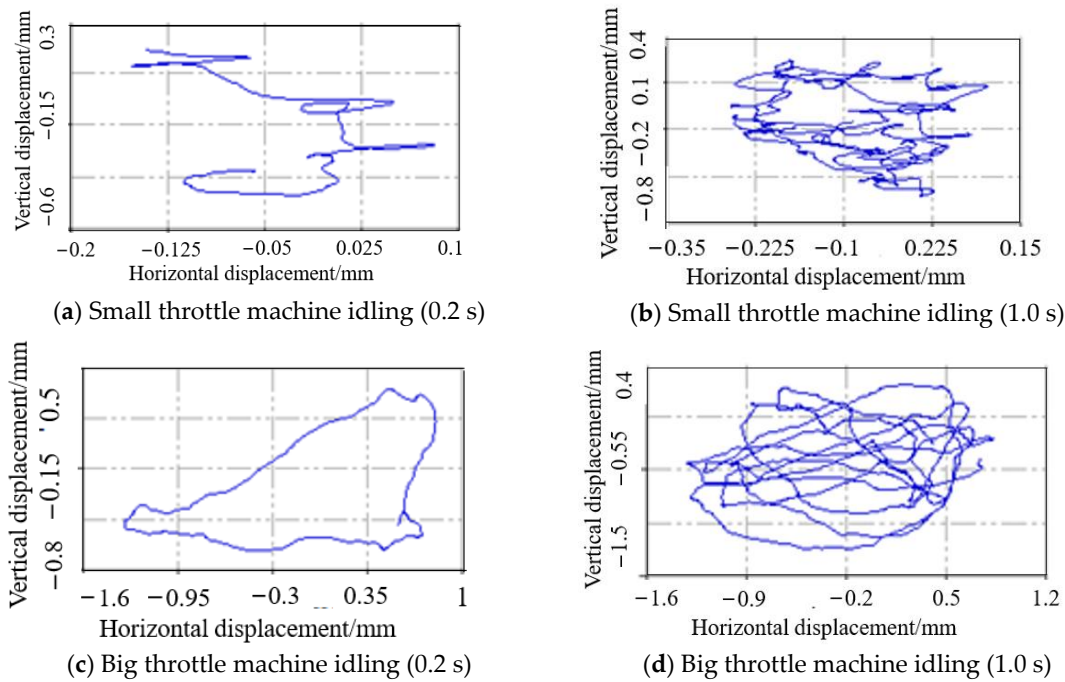


Figure 10. Axis locus of threshing cylinder without counterweight.

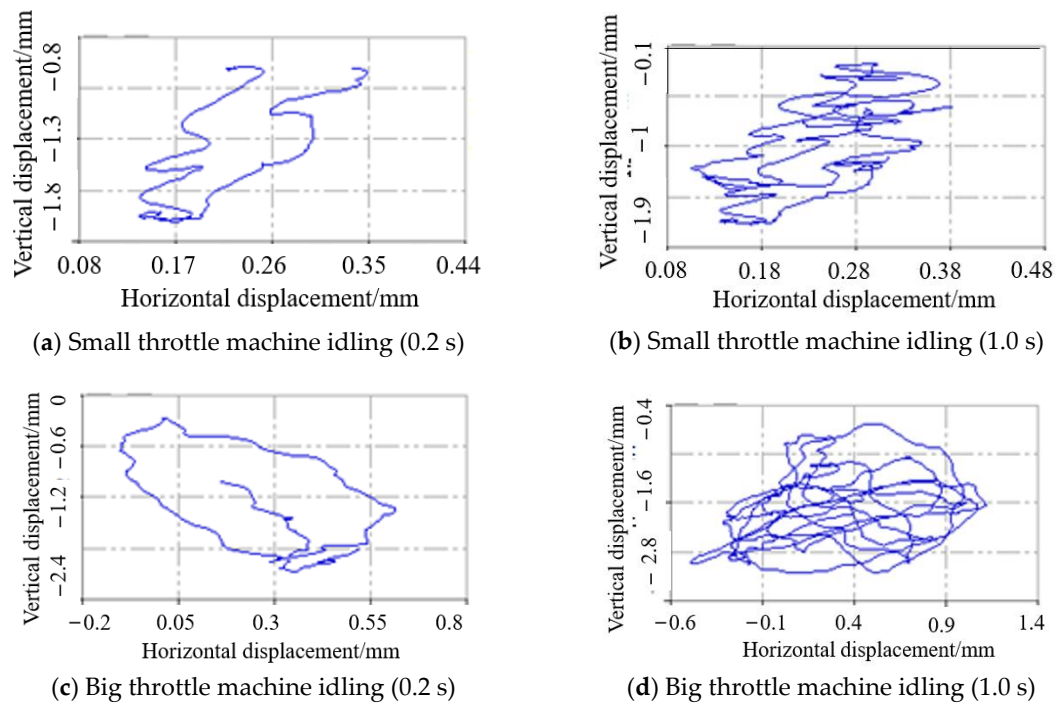


Figure 11. Axis locus of threshing cylinder under 200 g counterweight condition.

As can be seen from Figure 11 and Table 2, after the addition of 200 g counterweight, the horizontal displacement in the condition of small throttle increases with the increase in time. At the same time, the small throttle runs for 0.2 s compared with the small throttle which runs for 1.0 s. The data found that the little throttle runtime of the horizontal displacement is larger. However, whether it is a horizontal displacement or vertical displacement, the direction of the threshing drum is the same. In the gas state, the horizontal displacement can provide the largest change to 0.900 mm, and the minimum vertical displacement can reach 2.800 mm. As can be seen through the data, in comparison to 200 g of weight status

and light condition, the condition of vertical amplitude increases to 200 g, the horizontal amplitude decreases, and the vibration vector has not increased. At the same time, it can be found that the axis trajectory begins to concentrate around the direction with an angle of 45° from the horizontal and vertical directions, and a slight misalignment feature appears on the trajectory line.

**Table 2.** Add 200 g counterweight block threshing drum state.

Throttle Operating Condition	Horizontal Displacement	Vertical Displacement
Small throttle operation (0.2 s)	0.17	−1.8
	0.26	−1.3
	0.35	−0.8
Small throttle operation (1.0 s)	0.08	−1.9
	0.18	−1
	0.28	−0.1
High throttle operation (0.2 s)	0.05	−2.4
	0.3	−1.2
	0.55	−0.6
High throttle operation (1.0 s)	−0.1	−2.8
	0.4	−1.6
	0.9	−0.4

After the threshing drum added 400 g counterweight, the axis locus showed a more obvious “8” character, and the distribution law was similar to that when the threshing drum added 200 g counterweight. At this time, the threshing drum had a serious misalignment phenomenon, as shown in Figure 12.

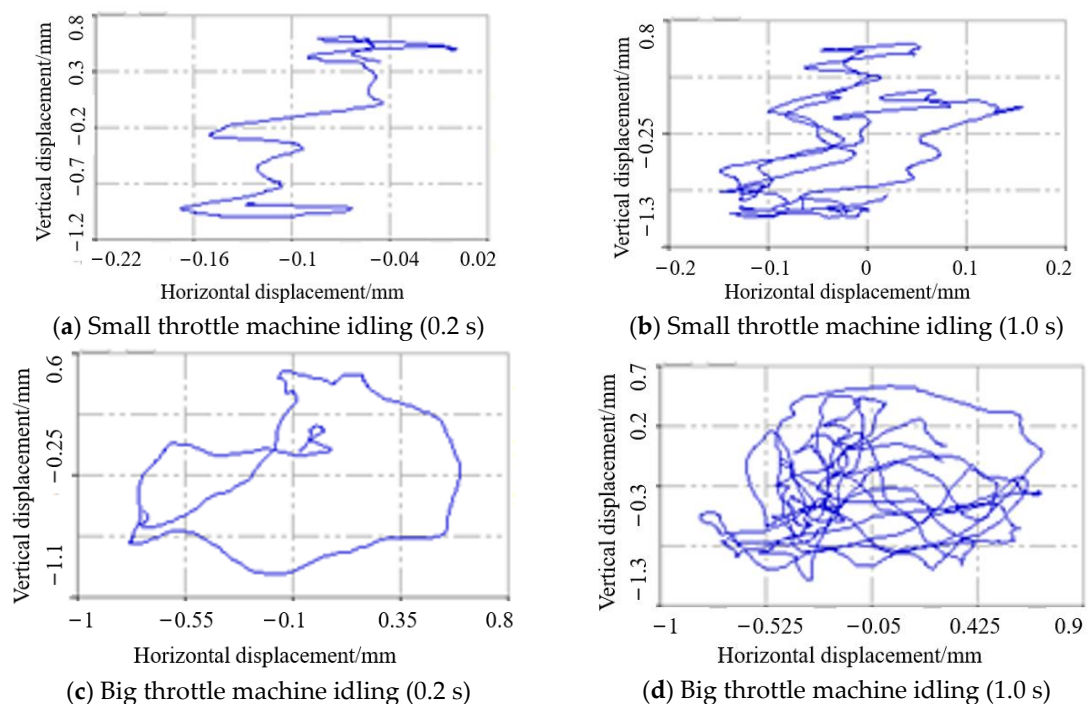


**Figure 12.** Axis locus of threshing cylinder under 400 g counterweight condition.

When 600 g of counterweight is added, it can be seen from Figure 13 that the axial locus displacement of the grain cylinder has been significantly gathered in the same direction during the operation of the small throttle, resulting in severe unbalanced vibration. However, the amplitude does not increase significantly, which is not much different from the amplitude of the rapid weight gain with the increase of 400 g.

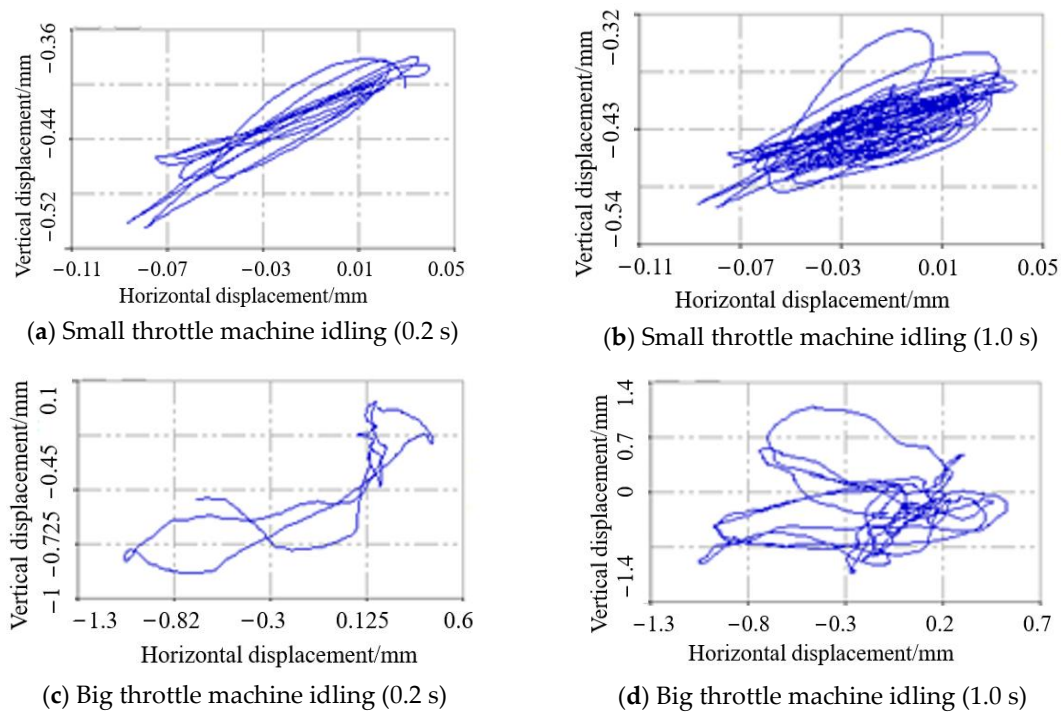


Figure 13. Axis locus of threshing cylinder under 600 g counterweight condition.

According to the analysis of Figure 13c,d, there are more spikes in the trajectory curve of the large throttle operation than that of the small throttle operation, indicating that the threshing cylinder is subjected to more intense friction during the large throttle operation. In the initial stage of rice feeding, the rice is continuously transferred from the feeding end to the threshing drum. At the same time, the weight of the stalk wrapped on the threshing rod teeth increases, which is similar to the process of increasing the counterweight; therefore the uneven distribution of rice along the threshing drum will enhance the unbalanced vibration of the threshing drum.

According to Figure 14, it can be seen intuitively that the amplitude of vertical displacement is larger than that of horizontal displacement, which can reach 0.54 mm while that of horizontal displacement can only reach 0.07. The amplitudes of horizontal displacement and vertical displacement decrease with the increase in running time in the small throttle operation state, while the amplitudes of horizontal displacement and vertical displacement increase with the increase in running time in the large throttle operation state. It can be found that with the gradual increase in axial counterweight, the eccentricity of threshing drum becomes more and more obvious. However, the amplitude did not increase significantly, which may be due to the small weight of the counterweight.

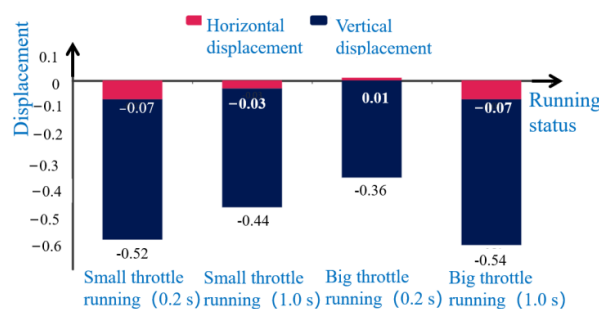
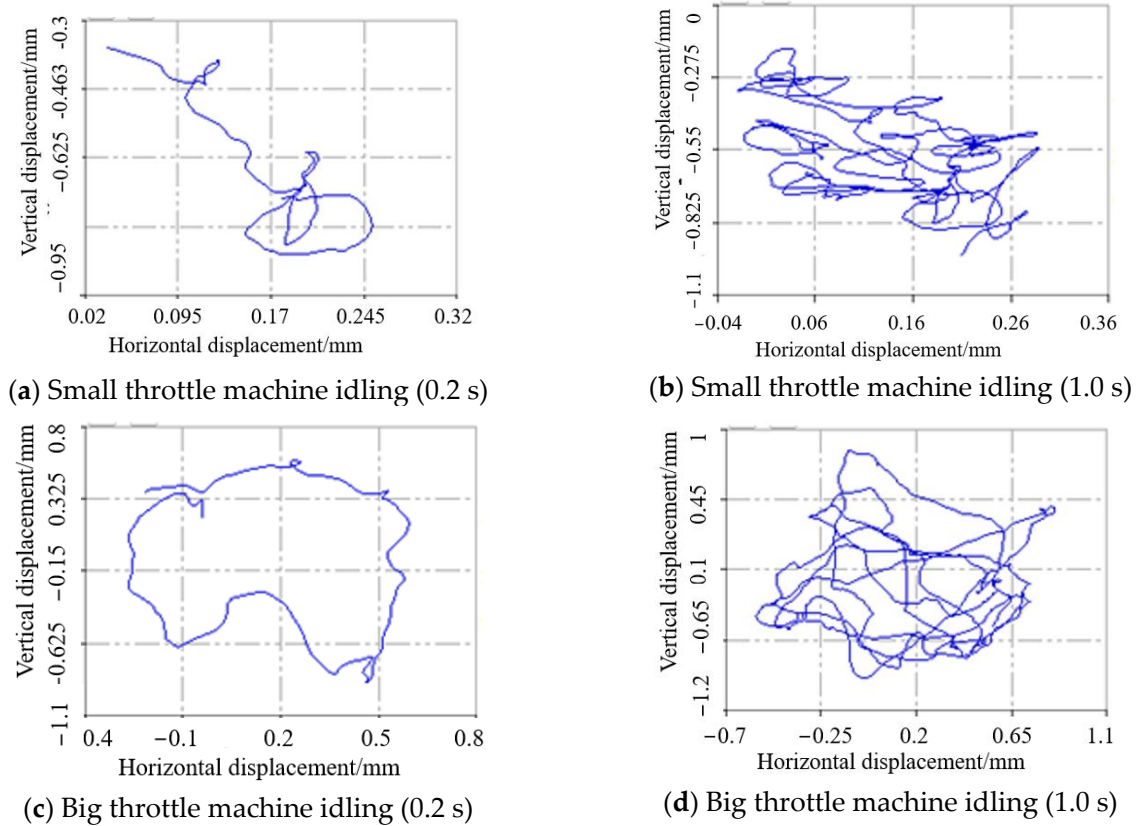


Figure 14. Displacement change in threshing drum under 600 g counterweight condition.

### 3.2. Influence of Stem Winding Radial Unbalance on Axis Locus of Threshing Drum

In order to study the influence of unbalanced vibration induced by stalk winding on threshing drum, the radial distribution test is needed. Similar to the coaxial distribution test it is divided into four groups for research. Among them, the axis locus measured by the no-load state of the first group and the addition of 200 g counterweight in the second group are respectively shown in Figures 10 and 11 in the coaxial distribution test, and the third and fourth groups are shown in Figures 15–18.



**Figure 15.** Axis locus of threshing drum under the condition of top cover 200 g and concave screen 200 g counterweight.

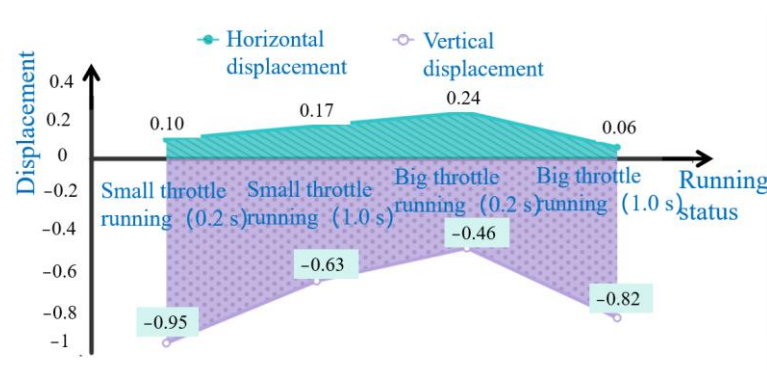


**Figure 16.** Displacement change in threshing drum under the top cover of 200 g and concave screen of 200 g.

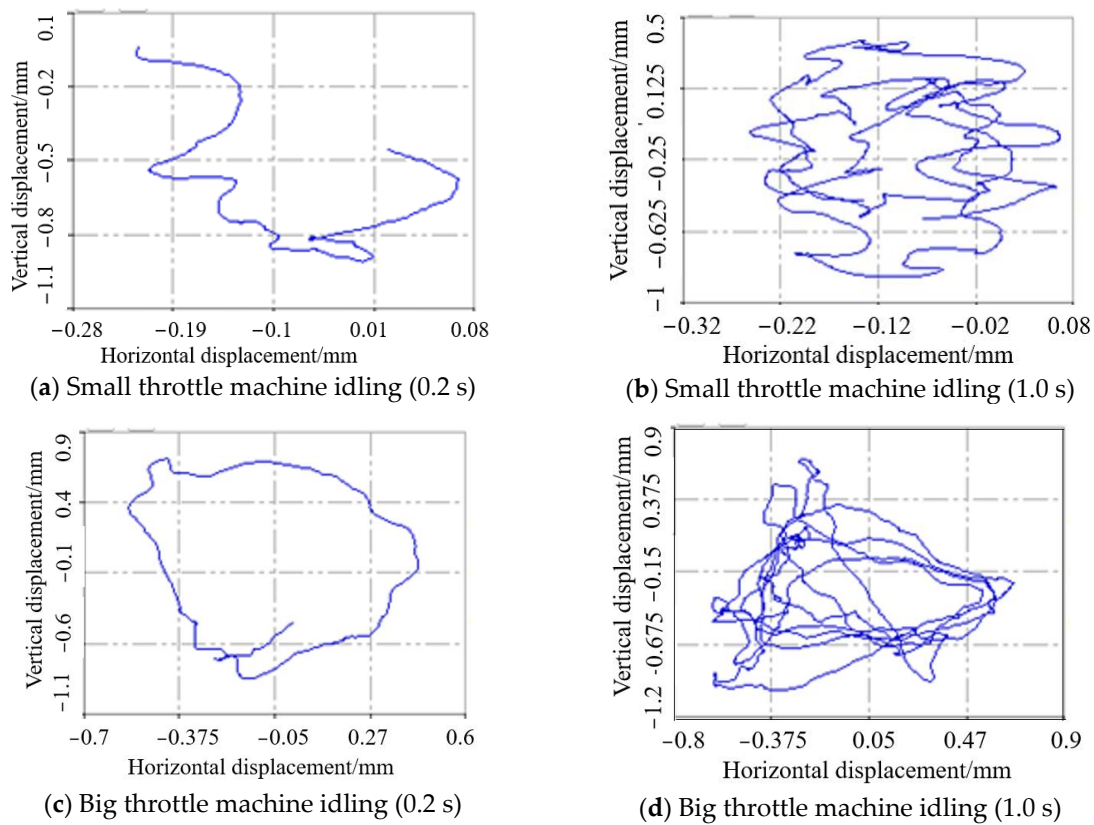


**Figure 17.** Track of threshing cylinder axis under the condition of 200 g top cover, 200 g concave plate screen, and 200 g balance weight between the top cover and concave plate screen.

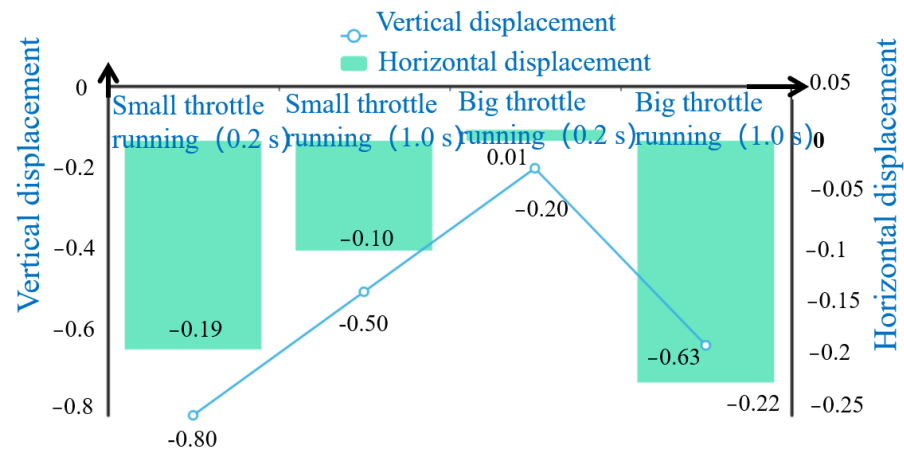


**Figure 18.** Displacement change in threshing drum with 200 g top cover, 200 g concave screen, and 200 g counterweight between the top cover and concave screen.

According to the original data, in the small throttle state, the horizontal amplitude can reach 0.300 mm and the vertical amplitude is 0.825 mm. In the high throttle state, the horizontal amplitude increases to 1.350 mm and the vertical amplitude increases to 1.650 mm. Compared with an increase of 200 g alone, both horizontal and vertical amplitudes are reduced. However, many “8” type features appear on the axis trajectory, indicating that the unbalanced masses located in different phases will partially cancel each other. In addition, the axis locus still has a tip, and the threshing drum is subject to local friction.

According to the Figure 16, you can see the change in the horizontal displacement and vertical displacement curve line, at the same time, the vertical displacement amplitude is greater than the horizontal displacement amplitude. In the condition of small throttle operation, the amplitude of both horizontal displacement and vertical displacement becomes smaller with the increase in running time, while in the condition of the large throttle operation, the amplitude of horizontal displacement and vertical displacement becomes smaller with the increase in running time. The amplitudes of both horizontal and vertical displacements increase. For the threshing drum, this will aggravate the unbalanced vibration of the threshing drum, and the threshing drum still has serious misalignment characteristics.

When running in a small throttle state, the horizontal amplitude reaches up to 0.300 mm, the vertical amplitude reaches up to 1.125 mm. When operating at high throttle, the horizontal amplitude increases to 1.275 mm and the vertical amplitude increases to 1.575 mm. The axial trajectory diagram is similar to Figure 15, which shows the general trend of the throttle operation state. From small throttle to large throttle, the horizontal displacement and vertical displacement first decrease and then increase, and the minimum and maximum values have a large span.

As can be seen from Figure 18, the vertical displacement fluctuates greatly, with a difference of 0.600 mm between the minimum and maximum amplitude, while the horizontal displacement fluctuates slightly, with a difference of 0.230 mm between the minimum and maximum amplitude. The horizontal displacement of the threshing drum is small in the small throttle operation, and larger in the large throttle operation, but it is still stable.

Through the analysis of Figures 17 and 18, it can be concluded that as the number of counterweights on the same circumference gradually increases, namely, the mass increases, the amplitude of the threshing drum does not increase, and the axis locus does not tend to converge in a certain area, but the characteristics of the mismatch become more and more obvious. According to the test results, it can be estimated that the uneven winding of the stalk on the radial of the threshing drum will aggravate the unbalanced vibration of the threshing drum during rice threshing, but it may not lead to an increase in amplitude.

#### 4. Conclusions

- (1) The axial locus test is carried out on the grain cylinder under no-load condition. When selecting a long vibration period, the axial locus of the central axis under no-load condition is mainly distributed in the second and fourth quadrangles of the coordinate system, indicating that the phase of the vibration of the central axis is opposite in the X and Z directions, even if the axial locus of the central axis is random. It still has a concentrated pulsating area. When a smaller vibration period is selected, the trajectories of the central axis are combined into a U-shape. The amplitude of the axis trajectory is constantly changing, but its trend and phase are roughly the same. Finally, it is concluded that the threshing drum runs stably under no-load condition.
- (2) The threshing drum under threshing condition was tested to analyze the change in axis locus, which provided a basis for the subsequent simulation of stalk winding distribution. The axis trajectory of the cylinder is also mainly concentrated in the second and fourth quadrant of the coordinate system, and the coordinates on the X and Z axes are opposite, similar to the axis trajectory of the central axis in the no-load state. However, in the threshed state, the amplitude obtained by the axis locus is more than 6 times larger than that in the no-load state, and the maximum amplitude is 559  $\mu\text{m}$ . It can be concluded that the vibration of threshing drum in threshing state is larger than that in no-load state.
- (3) To more accurately study the axial and radial distribution of the stem wrapped in the threshing drum, the counterweight block is used instead of the stem. It can be seen from the test results that the threshing cylinder as a whole is in a stable running state when there is no counterweight, but there is still friction in the local rotation. In the axial distribution test, with a weight of 200 g, the vertical amplitude increases

and the horizontal amplitude decreases. In the radial distribution test, it is found that after adding 400 g and 600 g counterweights, the horizontal and vertical amplitudes decrease, but the axis locus has more “8” character. Finally, it is concluded that as the mass increases, the amplitude of the threshing drum does not increase, and the axis locus does not converge in a certain area, but the characteristics of misalignment are more and more obvious.

**Author Contributions:** Conceptualization, Z.T.; methodology, Z.T. and T.W.; validation, Z.S., Z.D., and K.Q.; formal analysis, Z.T.; data curation, Z.S., Z.D., and T.W.; investigation, K.Q. and Z.S.; writing—original draft preparation, K.Q. and T.W.; writing—review and editing, K.Q., Z.D., and Z.S.; supervision, T.W. All authors have read and agreed to the published version of the manuscript.

**Funding:** This research work was supported by the National Natural Science Foundation of China (Grant No. 52175235), Key Laboratory of Intelligent Equipment and Robotics for Agriculture of Zhejiang Province (Grant No. 2023ZJZD2302), Key Laboratory of Modern Agricultural Equipment and Technology (Jiangsu University), Ministry of Education (MAET202326), Jiangsu Province and Education Ministry Co-sponsored Synergistic Innovation Center of Modern Agricultural Equipment (Grant No. XTCX2007), and the Key Laboratory of Modern Agricultural Equipment and Technology (Jiangsu University), Ministry of Education (MAET202109). A Project Funded by the Priority Academic Program Development of Jiangsu Higher Education Institutions (No. PAPD-2023-87).

**Data Availability Statement:** The data used to support the findings of this study are available from the corresponding author upon request.

**Conflicts of Interest:** Author Ting Wang was employed by the company Jiangsu World Agriculture Machinery Co., Ltd. The remaining authors declare that the research was conducted in the absence of any commercial or financial relationships that could be construed as a potential conflict of interest.

## References

1. Myhailovych, Y.; Rogovskii, I.; Korobko, M.; Berezova, L. Experimental studies of vibration load of synchronous threaded connections of grain harvester combines. *Eng. Rural Dev.* **2023**, *22*, 908–914.
2. Mohammadi, A.; Ghamary, B.; Jahanbakhshi, A.; Shahidi, R. Whole body vibration and driver response to ITM 475 Tractor. *Agric. Eng. Int. CIGR J.* **2023**, *25*.
3. Yang, S.W.; Hao, Y.X.; Zhang, W.; Yang, L.; Liu, L.T. Free vibration and buckling of eccentric rotating FG-GPLRC cylindrical shell using first-order shear deformation theory. *Compos. Struct.* **2021**, *263*, 113728. [[CrossRef](#)]
4. Geyer, T.F.; Kamps, L.; Sarradj, E.; Brücker, C. Vortex shedding and modal behavior of a circular cylinder equipped with flexible flaps. *Acta Acust. United Acust.* **2019**, *105*, 210–219. [[CrossRef](#)]
5. Abdi, S.; Abdi, E.; Toghiani, H.; McMahan, R. Vibration analysis of brushless doubly fed machines in the presence of rotor eccentricity. *IEEE Trans. Energy Convers.* **2020**, *35*, 1372–1380. [[CrossRef](#)]
6. Syahputra, M.N.A.F.; Subekti, S.; Indah, N. Effect of eccentric mass on rotor dynamics as a source of harvesting energy vibration. *JTTM J. Terap. Tek. Mesin* **2024**, *5*, 54–61.
7. Ogidi, O.O.; Barendse, P.S.; Khan, M.A. Detection of static eccentricity faults in AFPM machine with asymmetric windings using vibration analysis. In Proceedings of the International Conference on Electrical Machines, Berlin, Germany, 2–5 September 2014; pp. 1549–1554.
8. Umbataliyev, N.; Smailova, G.; Toilybayev, M.; Sansyzbayev, K.; Koshanova, S.; Bekmukhanbetova, S. Optimization of the technological process of threshing combine harvester. *East. -Eur. J. Enterp. Technol.* **2023**, *124*, 104. [[CrossRef](#)]
9. Lee, G.H.; Moon, B.E.; Basak, J.K.; Kim, N.E.; Paudel, B.; Jeon, S.W.; Kook, J.; Kang, M.Y.; Ko, H.J.; Kim, H.T. Assessment of load on threshing bar during soybean pod threshing. *J. Biosyst. Eng.* **2023**, *48*, 478–486. [[CrossRef](#)]
10. Bhandari, S.; Jotautienė, E. Vibration analysis of a roller bearing condition used in a tangential threshing drum of a combine harvester for the smooth and continuous performance of agricultural crop harvesting. *Agriculture* **2022**, *12*, 1969. [[CrossRef](#)]
11. Abdeen, M.A.; Xie, G.; Salem, A.E.; Fu, J.; Zhang, G. Longitudinal axial flow rice thresher feeding rate monitoring based on force sensing resistors. *Sci. Rep.* **2022**, *12*, 1369. [[CrossRef](#)]
12. Fouda, T.; Bahnas, O.; Soltan, M.; Ghoname, M. A study on threshing device wearing behavior for rice harvesting combine. Scientific Papers Series Management. *Econ. Eng. Agric. Rural Dev.* **2021**, *21*, 305–312.
13. Long, L.D. Mathematical model of the threshing process in a conventional combine-threshing. *J Agric Eng Res* **1982**, *2*, 119–130.
14. Nwuba, A.I.U.; Braide, F.G. Development of whole crop cowpea thresher as effected by grain and stalk properties. *J. Agric. Eng. Technol.* **1994**, *2*, 67–79.
15. Maertens, K.; De Baerdemaeker, J. Flow rate based prediction of threshing process in combine harvesters. *Appl. Eng. Agric.* **2003**, *19*, 383–388. [[CrossRef](#)]
16. Ndirika, V.I.O. Development and performance evaluation of a millet thresher. *J. Agric. Technol.* **1993**, *1*, 2–10.

17. Reina, S.; Ayabaca, C.; Venegas, D.; Zambrano, I.; Venegas, W.; Vila, C.; Ordoñez, V. Experimental validation in a controlled environment of a methodology for assessing the dynamic behavior of railway track components. *Machines* **2022**, *10*, 394. [[CrossRef](#)]
18. Heshmati, M. Influence of an eccentricity imperfection on the stability and vibration behavior of fluid-conveying functionally graded pipes. *Ocean Eng.* **2020**, *203*, 107192. [[CrossRef](#)]
19. Gabrielli, A.; Battarra, M.; Mucchi, E.; Dalpiaz, G. A procedure for the assessment of unknown parameters in modeling defective bearings through multi-objective optimization. *Mech. Syst. Signal Process.* **2023**, *185*, 109783. [[CrossRef](#)]
20. Alimardani, R.; Rahideh, A.; Hedayati-kia, S. Mixed eccentricity fault detection for induction motors based on time synchronous averaging of vibration signals. *IEEE Trans. Ind. Electron.* **2023**, *71*, 3173–3181. [[CrossRef](#)]
21. Syuhri, A.; Sholahuddin, I.; Syuhri, S.N.H.; Qoryah, R.D.H. Modeling and evaluation of a threshing drum under vertical vibration. *J. Mech. Eng. Sci.* **2018**, *12*, 3750–3758. [[CrossRef](#)]
22. Powar, R.V.; Aware, V.V.; Shahare, P.U. Optimizing operational parameters of finger millet threshing drum using RSM. *J. Food Sci. Technol.* **2019**, *56*, 3481–3491. [[CrossRef](#)] [[PubMed](#)]
23. Aneliak, M.; Kuzmych, A.; Stepanenko, S.; Lysaniuk, V. Study of the process of threshing leguminous grass seeds with a drum-type threshing device. *INMATEH-Agric. Eng.* **2023**, *71*, 83–92. [[CrossRef](#)]
24. Jotautienė, E.; Juostas, A.; Bhandari, S. Proper technical maintenance of combine harvester rolling bearings for smooth and continuous performance for grain crop agrotechnical requirements. *Appl. Sci.* **2021**, *11*, 8605. [[CrossRef](#)]
25. Fukushima, T.; Inoue, E.; Mitsuoka, M.; Okayasu, T.; Sato, K. Collision vibration characteristics with interspace in knife driving system of combine harvester. *Eng. Agric. Environ. Food* **2012**, *5*, 115–120. [[CrossRef](#)]
26. wooi Chuan, H.; Shek, J. Minimising unbalanced magnetic pull in doubly fed induction generators. *J. Eng.* **2019**, *2019*, 4008–4011.
27. Zastempowski, M.; Bochat, A. Gyroscopic effect in machine working assemblies. *Acta Technol. Agric.* **2020**, *23*, 24–29. [[CrossRef](#)]
28. Rawat, A.; Matsagar, V.A.; Nagpal, A.K. Free vibration analysis of thin circular cylindrical shell with closure using finite element method. *Int. J. Steel Struct.* **2020**, *20*, 175–193. [[CrossRef](#)]
29. Liu, Y.; Li, Y.; Zhang, T.; Huang, M. Effect of concentric and non-concentric threshing gaps on damage of rice straw during threshing for combine harvester. *Biosyst. Eng.* **2022**, *219*, 1–10. [[CrossRef](#)]
30. Ma, Z.; Wu, Z.; Li, Y.; Song, Z.; Yu, J.; Li, Y.; Xu, L. Study of the grain particle-conveying performance of a bionic non-smooth-structure screw conveyor. *Biosyst. Eng.* **2024**, *238*, 94–104. [[CrossRef](#)]
31. Liu, Y.; Li, Y.; Chen, L.; Zhang, T.; Liang, Z.; Huang, M.; Su, Z. Study on performance of concentric threshing device with multi-threshing gaps for rice combines. *Agriculture* **2021**, *11*, 1000. [[CrossRef](#)]
32. Liang, Z.; Li, J.; Liang, J.; Shao, Y.; Zhou, T.; Si, Z.; Li, Y. Investigation into experimental and DEM simulation of guide blade optimum arrangement in multi-rotor combine harvesters. *Agriculture* **2022**, *12*, 435. [[CrossRef](#)]
33. Ji, K.; Li, Y.; Liang, Z.; Liu, Y.; Cheng, J.; Wang, H.; Zhu, R.; Xia, S.; Zheng, G. Device and Method Suitable for Matching and Adjusting Reel Speed and Forward Speed of Multi-Crop Harvesting. *Agriculture* **2022**, *12*, 213. [[CrossRef](#)]
34. Li, Y.; Liu, Y.; Ji, K.; Zhu, R. A Fault Diagnosis Method for a Differential Inverse Gearbox of a Crawler Combine Harvester Based on Order Analysis. *Agriculture* **2022**, *12*, 1300. [[CrossRef](#)]
35. Lim, S.; Park, S.M.; Kim, K.I. AI vibration control of high-speed rotor systems using electrorheological fluid. *Shock Vib. Dig.* **2006**, *38*, 242–243. [[CrossRef](#)]
36. Huynh, V.M.; Powell, T.; Siddall, J.N. Threshing and separating process—A mathematical model. *Trans. ASAE* **1982**, *25*, 65–73. [[CrossRef](#)]

**Disclaimer/Publisher’s Note:** The statements, opinions and data contained in all publications are solely those of the individual author(s) and contributor(s) and not of MDPI and/or the editor(s). MDPI and/or the editor(s) disclaim responsibility for any injury to people or property resulting from any ideas, methods, instructions or products referred to in the content.